

This article may be downloaded for personal use only. Any other use requires prior permission of the author and AIP Publishing. This article appeared in *Chaos* 30, 053114 (2020); and may be found at: <https://doi.org/10.1063/1.5144709>

Copyright 2020 Author(s). This article is distributed under a Creative Commons Attribution 4.0 International (CC BY 4.0) License. <https://creativecommons.org/licenses/by/4.0/>

Derivation of a continuous time dynamic planar system with two unstable foci from a three-dimensional chaotic piecewise linear system

Cite as: Chaos **30**, 053114 (2020); <https://doi.org/10.1063/1.5144709>

Submitted: 10 January 2020 . Accepted: 16 April 2020 . Published Online: 07 May 2020

Eric Campos 



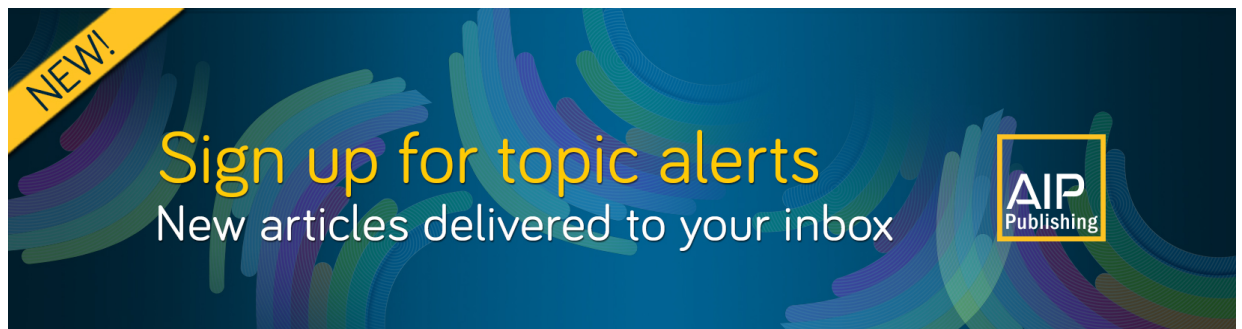
[View Online](#)



[Export Citation](#)



[CrossMark](#)



NEW!

Sign up for topic alerts
New articles delivered to your inbox

AIP
Publishing



Derivation of a continuous time dynamic planar system with two unstable foci from a three-dimensional chaotic piecewise linear system

Cite as: Chaos 30, 053114 (2020); doi: 10.1063/1.5144709

Submitted: 10 January 2020 · Accepted: 16 April 2020 ·

Published Online: 7 May 2020



View Online



Export Citation



CrossMark

Eric Campos^{a)} 

AFFILIATIONS

División de Matemáticas Aplicadas, Instituto Potosino de Investigación Científica y Tecnológica A. C., Camino a la Presa San José 2055, col. Lomas 4a Sección, 78216 San Luis Potosí, SLP, Mexico

^{a)}Author to whom correspondence should be addressed: eric.campos@ipicyt.edu.mx

ABSTRACT

In this paper, we introduce a class of continuous time dynamical planar systems that is capable of generating attractors in the plane by means of the use of hysteresis and at least two unstable foci. This class of systems shows stretching and folding behavior due to unstable equilibria and hysteresis. Hysteresis is used to overwhelm the constraints on the behavior of planar systems. This class of systems is derived from three-dimensional piecewise linear systems that have two manifolds, one stable and the other unstable, to generate heteroclinic chaos. Two numerical examples are given accordingly to the developed theory.

Published under license by AIP Publishing. <https://doi.org/10.1063/1.5144709>

The hysteresis phenomenon occurs widely in physics, chemistry, engineering, biology, economics, etc. For example, by plotting the current through the coil against the magnetic field of said coil, a hysteresis effect becomes visible. The dynamics projected onto a plane of a class of three-dimensional piecewise linear (PWL) systems is described by a class of planar systems based on hysteresis. The particular interest is to derive planar systems from a class of three-dimensional PWL systems that have an unstable saddle-focus in each subsystem.

I. INTRODUCTION

Chaos has been generated by continuous time three-dimensional PWL systems; for instance, the Chua's system is a chaotic PWL system that was reported in the literature.¹ PWL systems have been widely used to introduce several systems, for example, a generation of families of multiscroll attractors based on a modification of the Chua diode by adding breakpoints to its behavior.² A generation of chaos with only one type of stability of equilibria has been reported in Refs. 3 and 4. A characteristic is that

multiscroll attractors are generated by using only the saddle-focus point that generates scrolls in the Chua's system without including the saddle point between the two scrolls. Chaotic attractors without equilibria⁵⁻⁷ and deterministic Brownian motion^{8,9} have also been studied by means of PWL systems in \mathbb{R}^3 . Now, the interest is to introduce a PWL system in \mathbb{R}^2 capable of generating multiscroll attractors.

Systems involving PWL and based on the jerk equation and other systems have also been used to generate chaos. An overview of the breakthroughs on multiscroll chaotic attractor generation, including theories, methods, and applications, is given in Ref. 10. In Ref. 11, the authors introduced a generation of multiscroll attractors by means of the jerk equation and saturated function series and in Ref. 12 via a hysteresis series switching approach. A generation of multistable systems via dissipative systems with unstable dynamics is reported in Refs. 13 and 14. Therefore, these systems have a stable manifold responsible for system dissipation and another unstable manifold responsible for unstable dynamics. These kinds of systems have been used to present an approach to yield one-directional, two-directional, and three-directional grid multiscroll chaotic systems in \mathbb{R}^3 based on unstable dissipative systems via

a third-order differential equation.¹⁵ The aforementioned systems are some examples of the PWL system that let us know the great potential of these systems. In this work, the derived systems in \mathbb{R}^2 present, in each domain of the PWL system, an unstable manifold given by a focus equilibrium point that is responsible for the stretching of the flow, and the folding of trajectories is given by a hysteresis function.

Different physical implementations of systems with chaotic dynamics have allowed applications in different fields, such as medicine,¹⁶ biology, and several problems in electrical engineering.¹⁷ Therefore, experimental prototypes of chaotic PWL systems have allowed ascertaining the chaotic behavior and building applications based on chaos. For example, in Ref. 18, an analog electronic implementation by means of operational amplifiers of a class of hybrid dissipative systems in \mathbb{R}^3 is presented. Reference 19 introduces a 50-scroll chaotic attractor at 66 MHz by using field-programmable gate arrays (FPGAs). In Ref. 20, an experimental realization of a chaotic secure communication system is presented via Arduino's open source integrated development environment. In Ref. 21, a chaotic attractor is implemented by irregularly saturated nonlinear functions with an optimized positive Lyapunov exponent. Hyperchaotic dynamic has also been implemented by using the PWL system^{22–24} and applied to encryption schemes.²⁵

A hysteretic system displays a different response in a subspace of its phase space such that the magnitude of a resulting quantity is different during increases in the magnitude of the cause than during decreases. An analysis of two-dimensional PWL systems with hysteresis coming from a reduction of symmetric 3D systems with slow–fast dynamics is presented in Ref. 26 by considering hysteretic systems having two real equilibria of saddle type. Generation of multiscroll chaotic attractors from a given three-dimensional linear system via a hysteresis series controller has been reported in Refs. 27 and 28. Some experimental implementation of a chaotic generator via hysteresis has been proposed.^{29,30} In Ref. 31, an electronic chaos generator was proposed consisting of two capacitors, some resistors, one linear voltage-controlled current source (VCCS), and one PWL hysteresis VCCS. From Ref. 32, they applied the point transformation method of Andronov to analyze different kinds of oscillations that may occur in PWL systems with hysteresis.

There are two interesting trajectories that a dynamic system with equilibrium points in its vector field can present: heterocyclic orbits and homoclinic orbits. Recall that a path in the phase space that joins two different equilibrium points is called a *heteroclinic orbit*, and a path that starts and ends at the same point is called a *homoclinic orbit*. The famous Shil'nikov theorems showed that the existence of a homoclinic cycle or a heteroclinic cycle implies the existence of a countable number of horseshoes in a neighborhood of these cycles. Homoclinic and heteroclinic cycles can potentially result in chaos in dynamical systems. Shil'nikov proved that the existence of some kind of heteroclinic orbits (homoclinic orbits) implies that there are arbitrarily small perturbations of the vector field that have p -heteroclinic orbits (p -homoclinic orbits) and are, therefore, chaotic in a precise sense. The goal of many works has been to find the homoclinic or heteroclinic cycles in well-known systems. For example, in Ref. 33, homoclinic orbits and homoclinic chaos have been shown in a PWL Rössler-like circuit by numerical simulations; in Ref. 34, a numerical method is presented to demonstrate the

existence of homoclinic cycles or heteroclinic cycles in a PWL double-scroll circuit. On the other hand, some chaotic systems have been constructed to generate heteroclinic cycles to obtain heteroclinic chaos. In Ref. 35, sufficient conditions are given for the existence of heteroclinic cycles for a class of three-dimensional piecewise affine systems with a stable saddle-focus. Other chaotic systems are^{36,37} based on PWL systems that generate heteroclinic chaos.

Dissipative systems with unstable dynamics have been called unstable dissipative systems (UDS) of type I or II,³⁴ if they present a stable manifold of dimension one or two, respectively. This class of systems has been used to generate chaotic attractors based on heteroclinic orbits; therefore, heteroclinic chaos has been generated via PWL systems in Refs. 7 and 38. The characteristic of these previous works is that the generation of chaos is possible by using only one type of equilibria. Usually, the chaotic behavior of continuous time dynamical systems has been checked by using the Lyapunov exponents. The spectrum of Lyapunov exponents for continuous time systems in \mathbb{R}^3 presents a negative, a zero, and a positive Lyapunov exponent. Attractors with positive Lyapunov exponents are called a strange attractor. The positive Lyapunov exponent indicates exponential spreading within the attractor in the direction transverse to the flow, and the negative exponent indicates exponential contraction onto the attractor.

The topological horseshoe theory gives an approach to prove chaotic behavior in a dynamical system. The existence of a horseshoe in a dynamical system is a remarkable characteristic of chaos; due to this, there is a sequence of basic topological operations that consist of stretching and folding behavior. The former gives sensitivity to initial conditions and the second behavior gives the attraction.

There is an extensive list of continuous time dynamical systems that exhibit stretching and folding behavior in the space or greater dimensions, \mathbb{R}^n with $n \geq 3$. In this paper, we present a class of continuous time dynamical planar systems that shows stretching and folding behavior. This behavior is possible due to hysteresis being used to overwhelm the constraints on behavior of planar systems. The hysteresis phenomenon is characterized by its behavior that presents a response due to its current state and its past states. This allows having a different response for the same current state generating what it is called a hysteresis cycle.

This paper is organized as follows: In Sec. II, we present some definitions of PWL dynamical systems based on hysteresis. Section III contains some known results of heteroclinic chaos via PWL systems in \mathbb{R}^3 . In Sec. IV, we introduce a planar PWL system with two unstable foci and the generation of a double-scroll attractor. In Sec. V, an approach to derive PWL systems in \mathbb{R}^2 to generate multiscroll attractors is presented. Finally, the conclusions are given in Sec. VI.

II. PWL DYNAMICAL SYSTEM IN \mathbb{R}^2

Let $T: X \rightarrow X$ be a PWL system comprising two affine linear transformations of \mathbb{R}^2 acting on two convex sets defined as follows:

Definition 1: Let X be a subset of \mathbb{R}^2 and $\mathcal{D} = \{D_1, D_2\}$ be convex sets of X , such that $X = D_1 \cup D_2$, $D_1 \cap D_2 = H \neq \emptyset$, and $D_i - H \neq \emptyset$, with $i = 1, 2$.

Particularly, the convex sets are defined as follows:

$$D_1 = \{(x, y) : x < d_2 \in \mathbb{R}\} \quad \text{and} \\ D_2 = \{(x, y) : x > d_1 \in \mathbb{R}\}, \quad \text{with } d_1 < d_2.$$

We start by considering a PWL system T such that the action on each atom D_i , $i = 1, 2$, is determined by hysteresis. The so-called (delayed) relay is the simplest model of discontinuous hysteresis. A hysteresis is given by the following expression:

$$f_H(\mathbf{x}) = \begin{cases} s_1 & \text{while } \mathbf{x} \in D_1, \\ s_2 & \text{while } \mathbf{x} \in D_2. \end{cases} \quad (1)$$

This hysteresis expression needs to be initialized for $\mathbf{x}_0 \in H$; in our case, the initialization is given as follows:

$$f_H(\mathbf{x}_0) = \begin{cases} s_1 & \text{for } \mathbf{x}_0 \in D_1, \\ s_2 & \text{for } \mathbf{x}_0 \in D_2 - H. \end{cases} \quad (2)$$

A PWL system driven by a hysteresis is given as follows:

$$\dot{\mathbf{x}} = \begin{cases} A_1\mathbf{x} + B_1 & \text{for } f_H(\mathbf{x}) = s_1, \\ A_2\mathbf{x} + B_2 & \text{for } f_H(\mathbf{x}) = s_2, \end{cases} \quad (3)$$

where \mathbf{x} is the state vector of the system; each $A_i \in \mathbb{R}^{2 \times 2}$ is a nonsingular linear operator; each $B_i \in \mathbb{R}^2$ is a constant vector; and each atom D_i has an equilibrium point at $\mathbf{x}_i^* = -A_i^{-1}B_i$, with $i = 1, 2$. Our study is restricted to the same linear transformation, $A_1 = A_2$, and different vectors, $B_1 \neq B_2$.

Definition 2: The affine linear system $\dot{\mathbf{x}} = A\mathbf{x} + B$ is said to have an unstable focus at the equilibrium point \mathbf{x}^* if the matrix $A \in \mathbb{R}^{2 \times 2}$ has two complex conjugate eigenvalues $\lambda_{1,2}$ with a positive real part.

Let $\{v_1, v_2\}$ be a corresponding set of eigenvectors. Then, the unstable subspace E^u of the affine linear system $\dot{\mathbf{x}} = A\mathbf{x} + B$ with an unstable focus at \mathbf{x}^* is spanned by $\{v_1, v_2\}$.

The aim is to generate a PWL system based on two affine linear systems (A, B_i) , which have an unstable focus equilibrium point at $\mathbf{x}_i = -A^{-1}B_i$, with $i = 1, 2$. Notice that the system switches between two unstable subspaces E_i^u . Therefore, the role of the hysteresis is crucial in order to generate an attractor.

The class of PWL systems is given by (1)–(3) and by considering the following matrices and vectors:

$$A_1 = A_2 = \begin{pmatrix} \alpha & -\beta \\ \beta & \alpha \end{pmatrix}, B_1 = \begin{pmatrix} b_{11} \\ b_{12} \end{pmatrix}, B_2 = \begin{pmatrix} b_{21} \\ b_{22} \end{pmatrix}. \quad (4)$$

The idea is to determine a PWL system given by (1)–(3) from a PWL system in \mathbb{R}^3 that generates heteroclinic chaos; therefore, the approach is explained in Secs. III–VI.

III. HETEROCLINIC CHAOS

Consider the metric space X endowed with the Euclidean distance d . Let $T : X \rightarrow X$, with $X \subset \mathbb{R}^3$, be a PWL dynamical system whose dynamics is given by a family of sub-systems of the form

$$\dot{\mathbf{x}} = A\mathbf{x} + f(\mathbf{x})B, \quad (5)$$

where $\mathbf{x} = (x_1, x_2, x_3)^T \in \mathbb{R}^3$ is the state vector, $A = \{a_{ij}\} \in \mathbb{R}^{3 \times 3}$ is a nonsingular linear operator, $B = (b_1, b_2, b_3)^T$ is a constant vector, and f is a functional. The vector $f(\mathbf{x})B$ is a constant vector in

each atom P_i of a finite partition $\mathcal{P} = \{P_1, \dots, P_\eta\}$ ($\eta > 1$) of X , that is, $X = \bigcup_{1 \leq i \leq \eta} P_i$ and $P_i \cap P_j = \emptyset$ for $i \neq j$. Each atom contains a saddle-focus equilibrium point, and then there is a stable manifold and another unstable manifold. Therefore, the equilibria are given by $\mathbf{x}_{eq_i}^* = (x_{1eq_i}^*, x_{2eq_i}^*, x_{3eq_i}^*)^T = -f(\mathbf{x})A^{-1}B \in P_i$, with $i = 1, \dots, \eta$. The switching surface between a pair of atoms, P_i and P_j , is given by the intersection of the closure of them, i.e., $SW_{ij} = cl(P_i) \cap cl(P_j)$.

To induce oscillations of the flow around the equilibria $\mathbf{x}_{eq_i}^*$, it is necessary to assign a negative real eigenvalue $\lambda_1 = \gamma$ to matrix A with the corresponding eigenvector v_1 and a pair of complex conjugate eigenvalues with a positive real part, $\lambda_2 = \alpha + i\beta$ and $\lambda_3 = \alpha - i\beta$, with the corresponding eigenvectors v_2 and v_3 . Thus, the stable and unstable manifolds are given by

$$W_{\mathbf{x}_{eq_i}^*}^s = \{\mathbf{x} + \mathbf{x}_{eq_i}^* \in P_i : \mathbf{x} \in span\{v_1\}\}$$

and

$$W_{\mathbf{x}_{eq_i}^*}^u = \{\mathbf{x} + \mathbf{x}_{eq_i}^* \in P_i : \mathbf{x} \in span\{v_2, v_3\}\},$$

with $i = 1, \dots, \eta$. These sets generate the contraction and expansion of the trajectories that are necessary for chaotic dynamics.

Assumption 1: The switching planes $SW_{ij} = cl(P_i) \cap cl(P_j)$ pass through the intersection points $cl(W_{\mathbf{x}_{eq_i}^*}^u) \cap W_{\mathbf{x}_{eq_j}^*}^s \neq \emptyset$ and $cl(W_{\mathbf{x}_{eq_j}^*}^u) \cap W_{\mathbf{x}_{eq_i}^*}^s \neq \emptyset$ of two adjacent atoms P_i and P_j , with $j = i + 1$ and $i = 1, 2, \dots, \eta - 1$; $cl(W_{\mathbf{x}_{eq_i}^*}^u) \cap W_{\mathbf{x}_{eq_j}^*}^s \in P_j$, and $cl(W_{\mathbf{x}_{eq_j}^*}^u) \cap W_{\mathbf{x}_{eq_i}^*}^s \in P_i$.

Notice that Assumption 1 implies $SW_{ij} \cap W_{\mathbf{x}_{eq_i}^*}^s \neq \emptyset$ and $SW_{ij} \cap W_{\mathbf{x}_{eq_j}^*}^s \neq \emptyset$.

One of the most important and useful mathematical constructs is the “ ∇ operator.” The dot product of ∇ and a vector field \vec{F} gives a scalar, known as the divergence of \vec{F} , for each point in the space. The volume rate of a flow through a source or sink is equal to the divergence of the vector field, i.e., with the flow through a sink given a negative sign in the divergence. A system that presents a negative divergence is called dissipative.

Assumption 2: The divergence of the PWL system (5) considering the linear operator A defined above is $\nabla = 2\alpha + \gamma$; therefore, the system is dissipative in each atom of the partition \mathcal{P} if $2\alpha < |\gamma|$.

Definition 3: The PWL system (5) is said to be an Unstable Dissipative System (UDS) if the system is dissipative with unstable dynamics determined by the eigenvalues of the linear operator A as follows: a real eigenvalue $\lambda_1 = \gamma$ and a pair of complex conjugate eigenvalues $\lambda_2 = \alpha + i\beta$ and $\lambda_3 = \alpha - i\beta$, such that $\nabla = 2\alpha + \gamma < 0$. If the stability index is one or two, then the UDS is type I or II, respectively.

The manifolds are responsible for connecting the equilibria of this class of dynamical systems. At least two equilibria are necessary to generate a heteroclinic orbit; therefore, we start by considering a partition with two atoms $\mathcal{P} = \{P_1, P_2\}$ and the constant vector $B \in \mathbb{R}^3$, and the functional f is given by

$$f(\mathbf{x}) = \begin{cases} \kappa_1, & \mathbf{x} \in P_1, \\ \kappa_2, & \mathbf{x} \in P_2, \end{cases} \quad (6)$$

with $\kappa_1, \kappa_2 \in \mathbb{R}$.

A switching surface SW will be a hyperplane oriented by its positive normal. SW divides \mathbb{R}^3 into two connected components; if a point \mathbf{x} lies in the component pointed by the positive normal of SW , we will write $\mathbf{x} > SW$. Also, $\mathbf{x} < SW$ if it lies in the other component but not in the plane SW . According to Assumption 1, the points $cl(W_{\mathbf{x}_{eq1}^*}^u) \cap W_{\mathbf{x}_{eqj}^*}^s \in P_j$ and $cl(W_{\mathbf{x}_{eqj}^*}^u) \cap W_{\mathbf{x}_{eqi}^*}^s \in P_i$ belong to different atoms but are in the same SW . Therefore, SW is split by two sets SW^- and SW^+ .

In the same spirit that in Ref. 39, the next proposition gives the necessary and sufficient conditions to generate heteroclinic connections between equilibria of a PWL dynamical system. Thus, the emergence of a chaotic attractor in this type of systems is possible.

Proposition 3: *The hyperbolic system given by (5) and (6) generates a pair of heteroclinic orbits if the system is UDS type I and the switching plane is given according to Assumption 1.*

Proof. Each trajectory with the initial condition $\mathbf{x}_0 \in W_{\mathbf{x}_{eq1}^*}^s$ tends to the equilibrium point \mathbf{x}_{eq1}^* ; therefore, $\varphi(\mathbf{x}_0, t) \rightarrow \mathbf{x}_{eq1}^*$ as $t \rightarrow \infty$. There is a set $\Gamma_1^s \subset W_{\mathbf{x}_{eq1}^*}^s$ given by the points located between the equilibrium point \mathbf{x}_{eq1}^* and the point $cl(W_{\mathbf{x}_{eq2}^*}^s) \cap cl(W_{\mathbf{x}_{eq1}^*}^u)$ so that each trajectory with the initial condition $\mathbf{x}_0 \in \Gamma_1^s$ tends to the point $cl(W_{\mathbf{x}_{eq2}^*}^s) \cap cl(W_{\mathbf{x}_{eq1}^*}^u)$ in back time, i.e., $\varphi(\mathbf{x}_0, t) \rightarrow cl(W_{\mathbf{x}_{eq1}^*}^s) \cap cl(W_{\mathbf{x}_{eq2}^*}^u)$ as $t \rightarrow -\infty$.

On the other hand, there is a set $\Gamma_2^u \subset W_{\mathbf{x}_{eq2}^*}^u$ such that each trajectory with initial condition $\mathbf{x}_0 \in \Gamma_2^u$ converges to the point $cl(W_{\mathbf{x}_{eq1}^*}^s) \cap cl(W_{\mathbf{x}_{eq2}^*}^u)$; i.e., if $\mathbf{x}_0 \in \Gamma_2^u \subset W_{\mathbf{x}_{eq2}^*}^u$, then $\varphi(\mathbf{x}_0, t) \rightarrow cl(W_{\mathbf{x}_{eq1}^*}^s) \cap cl(W_{\mathbf{x}_{eq2}^*}^u)$ as $t \rightarrow \infty$. The aforementioned statement is true because of Assumption 1. Because all trajectories with the initial condition $\mathbf{x}_0 \in W_{\mathbf{x}_{eq2}^*}^u$ converge to the equilibrium point \mathbf{x}_{eq2}^* in back time, i.e., $\varphi(\mathbf{x}_0, t) \rightarrow \mathbf{x}_{eq2}^*$ as $t \rightarrow -\infty$, then Γ_2^u is defined as the set comprising the points $\mathbf{x}_0 \in W_{\mathbf{x}_{eq2}^*}^u$ such that $\varphi(\mathbf{x}_0, t) \rightarrow \mathbf{x}_{eq2}^*$ as $t \rightarrow -\infty$ and $\varphi(\mathbf{x}_0, t) \rightarrow cl(W_{\mathbf{x}_{eq1}^*}^s) \cap cl(W_{\mathbf{x}_{eq2}^*}^u)$ as $t \rightarrow \infty$.

Therefore, the heteroclinic orbit HO_{21} from the equilibrium point \mathbf{x}_{eq2}^* to the equilibrium point \mathbf{x}_{eq1}^* is given by the set $\Gamma_1^s \cup \Gamma_2^u$. Then, we could also express the heteroclinic orbit as

$$HO_{21} = \{\mathbf{x} \in \varphi(\mathbf{x}_0, t) : \mathbf{x}_0 \in \Gamma_2^u \wedge t \in (-\infty, 0]\} \cup \{\mathbf{x} \in \varphi(\mathbf{x}_0, t) : \mathbf{x}_0 \in \Gamma_1^s \wedge t \in [0, \infty)\}.$$

In a similar way, it is possible to identify two sets $\Gamma_2^s \subset W_{\mathbf{x}_{eq2}^*}^s$ and $\Gamma_1^u \subset W_{\mathbf{x}_{eq1}^*}^u$, such that each trajectory with the initial condition $\mathbf{x}_0 \in \Gamma_2^s$ fulfills $\varphi(\mathbf{x}_0, t) \rightarrow cl(W_{\mathbf{x}_{eq2}^*}^s) \cap cl(W_{\mathbf{x}_{eq1}^*}^u)$ as $t \rightarrow -\infty$. Also, each trajectory with the initial condition $\mathbf{x}_0 \in \Gamma_1^u$ fulfills $\varphi(\mathbf{x}_0, t) \rightarrow cl(W_{\mathbf{x}_{eq2}^*}^s) \cap cl(W_{\mathbf{x}_{eq1}^*}^u)$ as $t \rightarrow \infty$. Therefore, the heteroclinic orbit HO_{12} from the equilibrium point \mathbf{x}_{eq1}^* to the equilibrium point \mathbf{x}_{eq2}^* is given by the set $\Gamma_2^s \cup \Gamma_1^u$. Then, we could also express the heteroclinic orbit as

$$HO_{12} = \{\mathbf{x} \in \varphi(\mathbf{x}_0, t) : \mathbf{x}_0 \in \Gamma_1^u \wedge t \in (-\infty, 0]\} \cup \{\mathbf{x} \in \varphi(\mathbf{x}_0, t) : \mathbf{x}_0 \in \Gamma_2^s \wedge t \in [0, \infty)\}.$$

□

The aforementioned Proposition 3 warrants that there exist initial conditions $\mathbf{x}_{01}, \mathbf{x}_{02} \in SW$, such that two solution curves $\varphi(\mathbf{x}_{01}, t)$ and $\varphi(\mathbf{x}_{02}, t)$ of the hyperbolic system given by (5) and (6) fulfill that $\varphi(\mathbf{x}_{01}, t) \rightarrow \mathbf{x}_{eq1}^*$ and $\varphi(\mathbf{x}_{02}, t) \rightarrow \mathbf{x}_{eq2}^*$ as $t \rightarrow \infty$ and $\varphi(\mathbf{x}_{01}, t) \rightarrow \mathbf{x}_{eq2}^*$ and $\varphi(\mathbf{x}_{02}, t) \rightarrow \mathbf{x}_{eq1}^*$ as $t \rightarrow -\infty$; in particular, these initial conditions correspond to the intersection points $cl(W_{\mathbf{x}_{eq1}^*}^s) \cap cl(W_{\mathbf{x}_{eq2}^*}^u)$ and $cl(W_{\mathbf{x}_{eq2}^*}^s) \cap cl(W_{\mathbf{x}_{eq1}^*}^u)$.

The following proposition is a direct consequence of Proposition 3.

Proposition 4: *If the partition \mathcal{P} contains more than two atoms $\{P_1, P_2, \dots, P_k\}$, with $2 < k \in \mathbb{Z}^+$, and each atom is a hyperbolic set defined as above. Furthermore, the atoms by pairs P_i and P_{i+1} fulfill Proposition 3. Then, the system generates $2(k - 1)$ heteroclinic orbits.*

This Proposition 4 warrants multiple heteroclinic orbits to generate multiscroll attractors under the below assumption.

Assumption 5: *The oscillations around the equilibrium point \mathbf{x}_{eqi}^* depend on parameters α and β , and we consider $\beta/\alpha \geq 10$.*

The trajectory $\mathbf{x}(t)$ of the PWL system can be calculated by $\mathbf{x}^i(t) = e^{At} \mathbf{x}_0^i$ in each atom P_i , where $\mathbf{x}^i = \mathbf{x} + \mathbf{x}_{eqi}^*$ and \mathbf{x}_0^i is the initial condition when the trajectory enters the atom P_i , $i = 1, 2$. Then,

$$\mathbf{x}^i(t) = QE(t)Q^{-1}\mathbf{x}^i(0),$$

where Q is the invertible matrix defined by the eigenvectors of A ; therefore, $E(t)$ is given by one of the following forms:

$$E(t) = \begin{pmatrix} e^{\gamma t} & 0 & 0 \\ 0 & e^{\alpha t} \cos(\beta t) & -e^{\alpha t} \sin(\beta t) \\ 0 & e^{\alpha t} \sin(\beta t) & e^{\alpha t} \cos(\beta t) \end{pmatrix} \quad (7)$$

or

$$E(t) = \begin{pmatrix} e^{\alpha t} \cos(\beta t) & -e^{\alpha t} \sin(\beta t) & 0 \\ e^{\alpha t} \sin(\beta t) & e^{\alpha t} \cos(\beta t) & 0 \\ 0 & 0 & e^{\gamma t} \end{pmatrix}. \quad (8)$$

The flow of the system $\varphi(\mathbf{x}_0)$ is dissipative in each atom for all initial conditions $\mathbf{x}_0 \in P_i - W_{\mathbf{x}_{eqi}^*}^u \subset X$.

As an example, we consider the system (5) and (6) that was given in Ref. 39 with the switching surface and parameters α, β, γ , and κ as follows:

Example 1: *A PWL system to generate heteroclinic chaos by considering a partition with two atoms $\mathcal{P} = \{P_1, P_2\}$, where $P_1 = \{\mathbf{x} \in \mathbb{R}^3 : \mathbf{x} < SW \text{ or } \mathbf{x} \in SW^-\}$ and $P_2 = \{\mathbf{x} \in \mathbb{R}^3 : \mathbf{x} > SW \text{ or } \mathbf{x} \in SW^+\}$, with the switching plane $SW = \{\mathbf{x} \in \mathbb{R}^3 : 2x_1 - x_3 = 0\}$, $SW^- = \{\mathbf{x} \in \mathbb{R}^3 : x_3 \geq 0\} \cap SW$, and $SW^+ = \{\mathbf{x} \in \mathbb{R}^3 : x_3 < 0\} \cap SW$, and the parameters $\alpha = 0.2, \beta = 5, \gamma = -3, \kappa_1 = -1$, and $\kappa_2 = 1$.*

The matrix of the linear operator $A \in \mathbb{R}^{3 \times 3}$ and the constant vector $B \in \mathbb{R}^3$ based on the eigenvalues are defined in Ref. 39 as follows:

$$A = \begin{pmatrix} \frac{\alpha}{3} + \frac{2\gamma}{3} & \beta & \frac{2\gamma}{3} - \frac{2\alpha}{3} \\ -\frac{\beta}{3} & \alpha & \frac{2\beta}{3} \\ \frac{\gamma}{3} - \frac{\alpha}{3} & -\beta & \frac{2\alpha}{3} + \frac{\gamma}{3} \end{pmatrix}, B = \begin{pmatrix} -\frac{\alpha}{3} - \frac{2\gamma}{3} \\ \frac{\beta}{3} \\ \frac{\alpha}{3} - \frac{\gamma}{3} \end{pmatrix}, \quad (9)$$

whose eigenvectors are

$$v_1 = \begin{pmatrix} 1 \\ 0 \\ \frac{1}{2} \end{pmatrix}, v_2 = \begin{pmatrix} 0 \\ -1 \\ 0 \end{pmatrix}, v_3 = \begin{pmatrix} -1 \\ 0 \\ 1 \end{pmatrix}. \quad (10)$$

Therefore, the equilibria are at $\mathbf{x}_{eq1}^* = (-1, 0, 0)^T \in P_1$ and $\mathbf{x}_{eq2}^* = (1, 0, 0)^T \in P_2$, and the stable and the unstable manifolds are given by

$$W_{\mathbf{x}_{eq1}^*}^u = \{\mathbf{x} \in \mathbb{R}^3 : x_1 + x_3 + 1 = 0\},$$

$$W_{\mathbf{x}_{eq2}^*}^u = \{\mathbf{x} \in \mathbb{R}^3 : x_1 + x_3 - 1 = 0\},$$

$$W_{\mathbf{x}_{eq1}^*}^s = \left\{ \mathbf{x} \in \mathbb{R}^3 : \frac{x_1 + 1}{2} = x_3; x_2 = 0 \right\},$$

and

$$W_{\mathbf{x}_{eq2}^*}^s = \left\{ \mathbf{x} \in \mathbb{R}^3 : \frac{x_1 - 1}{2} = x_3; x_2 = 0 \right\}.$$

The intersection points are given by $cl(W_{\mathbf{x}_{eq2}^*}^s) \cap cl(W_{\mathbf{x}_{eq1}^*}^u) = (-\frac{1}{3}, 0, -\frac{2}{3})^T$, $cl(W_{\mathbf{x}_{eq1}^*}^s) \cap cl(W_{\mathbf{x}_{eq2}^*}^u) = (\frac{1}{3}, 0, \frac{2}{3})^T$.

The above defined system fulfills Proposition 3; therefore, it presents a heteroclinic orbit [see Fig. 1(a)]. Then, heteroclinic chaos emerges from this system; in particular, a double-scroll attractor is generated as it is shown in Fig. 1(b), for the following initial condition $\mathbf{x}_0 = (0, 0, 0)^T$, and Fig. 2 shows projections of the double-scroll attractor onto different planes: (a) (x_1, x_2) , (b) (x_1, x_3) , and (c) (x_2, x_3) .

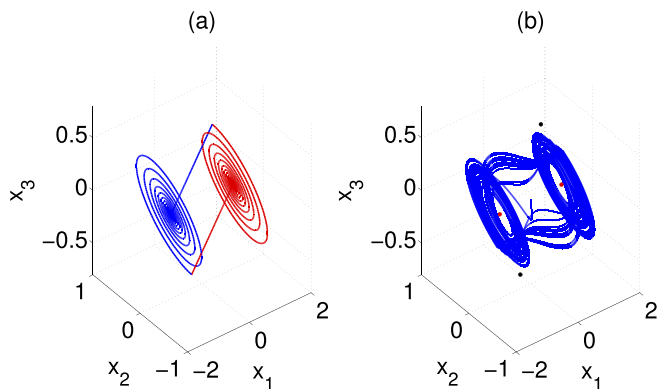


FIG. 1. (a) Heteroclinic cycle, the blue and red trajectories belong to the atoms P_1 and P_2 , respectively. The heteroclinic orbit from \mathbf{x}_{eq1}^* to \mathbf{x}_{eq2}^* is comprised of the blue spiral trajectory and the red straight trajectory. Another heteroclinic orbit from \mathbf{x}_{eq2}^* to \mathbf{x}_{eq1}^* is comprised of the red spiral trajectory and the blue straight trajectory. (b) A double-scroll attractor that emerges from a heteroclinic orbit using the following initial condition $\mathbf{x}_0 = (0, 0, 0)^T$ and the parameters $\alpha = 0.2, \beta = 5, \gamma = -3, \kappa_1 = -1, \kappa_2 = 1$ for the system defined by (5) and (6) with the switching surface $SW = \{\mathbf{x} \in \mathbb{R}^3 : 2x_1 - x_3 = 0\}$. The equilibria, \mathbf{x}_{eq1}^* and \mathbf{x}_{eq2}^* , are marked in red dots, and the black dots correspond to the intersection of the blue and red trajectories of (a).

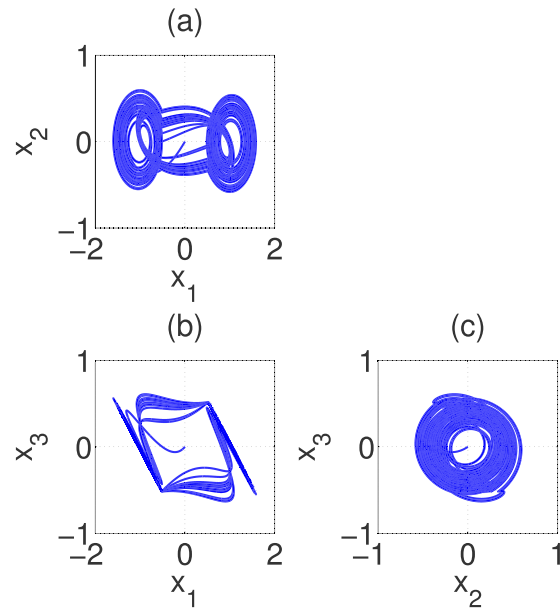


FIG. 2. Projections of the double-scroll attractor on the planes: (a) (x_1, x_2) , (b) (x_1, x_3) , and (c) (x_2, x_3) . The initial condition is $\mathbf{x}_0 = (0, 0, 0)^T$ and the parameters $\alpha = 0.2, \beta = 5, \gamma = -3, \kappa_1 = -1, \kappa_2 = 1$ for the system defined by (5) and (6) with the switching surface $SW = \{\mathbf{x} \in \mathbb{R}^3 : 2x_1 - x_3 = 0\}$.

IV. DERIVATION OF A CONTINUOUS TIME DYNAMIC PLANAR SYSTEM WITH TWO UNSTABLE FOCI

In this section, we derive a PWL system in \mathbb{R}^2 by reducing the affine linear system (5) to an uncoupled affine linear system, and the linear transformation of coordinates is defined by

$$\mathbf{y} = Q^{-1}\mathbf{x},$$

$$\dot{\mathbf{y}} = Q^{-1}A Q \mathbf{y} + Q^{-1}f(Q\mathbf{y})B, \quad (11)$$

where $\mathbf{y} = (y_1, y_2, y_3)^T \in \mathbb{R}^3$ is the state vector of the uncoupled system. From (11), the linear operator $A \in \mathbb{R}^{3 \times 3}$ can be expressed as

$$A = QEQ^{-1}, \quad (12)$$

where $Q = [v_1 \ v_2 \ v_3]$. Also, E is given by one of the following forms:

$$E = \begin{pmatrix} \gamma & 0 & 0 \\ 0 & \alpha & -\beta \\ 0 & \beta & \alpha \end{pmatrix} \quad \text{or} \quad E = \begin{pmatrix} \alpha & -\beta & 0 \\ \beta & \alpha & 0 \\ 0 & 0 & \gamma \end{pmatrix}; \quad (13)$$

thus, system (11) can be expressed as

$$\dot{\mathbf{y}} = E\mathbf{y} + Q^{-1}f(Q\mathbf{y})B. \quad (14)$$

A continuous time dynamic planar system with two unstable foci is derived from (13), which is as follows. The matrices $A_1, A_2 \in \mathbb{R}^{2 \times 2}$ of the system (3) are defined from the Jordan canonical form. Particularly, they are given by the Jordan block related to

the complex eigenvalues $\lambda_2 = \alpha + i\beta$ and $\lambda_3 = \alpha - i\beta$ of $A \in \mathbb{R}^{3 \times 3}$. Then,

$$A_1 = A_2 = \begin{pmatrix} \alpha & -\beta \\ \beta & \alpha \end{pmatrix}. \tag{15}$$

The planar system (3) and the hysteresis are defined by (1) and (2). Without loss of generality, the planar PWL system, for $0 < t \in \mathbb{R}$, is given by

$$\dot{\mathbf{x}} = \begin{cases} A_1 \mathbf{x} + B_1 & \text{while } \mathbf{x} \in D_1, \\ A_2 \mathbf{x} + B_2 & \text{while } \mathbf{x} \in D_2, \end{cases} \tag{16}$$

where $\mathbf{x} = (x, y)^T$ is the state vector of the system and $B_1, B_2 \in \mathbb{R}^2$ are constant vectors. The equilibria of the system, $\mathbf{x}_1^* = (x_1^*, y_1^*)^T \in D_1$ and $\mathbf{x}_2^* = (x_2^*, y_2^*)^T \in D_2$, are determined by the components of the equilibria given by \mathbf{y}_{eq1}^* and \mathbf{y}_{eq2}^* according to the Jordan block related to the complex eigenvalues. For instance, if we consider the first matrix E given by (13), then the equilibria \mathbf{x}_1^* and \mathbf{x}_2^* are given by the second and third components, respectively. The borders of the convex sets D_1 and D_2 , where subsystems (A_1, B_1) and (A_2, B_2) are acting, are given by two lines l_1 and l_2 that pass through the equilibria \mathbf{x}_1^* and \mathbf{x}_2^* , respectively. These lines l_1 and l_2 are parallel to the projected line given by the intersection of the plane QSW with the unstable manifold, where QSW is the switching plane SW transformed by Q . Finally, the vectors B_1 and B_2 are defined by $-A_1 \mathbf{x}_1^*$ and $-A_2 \mathbf{x}_2^*$, respectively.

Proposition 6: *If a PWL system is given by (5) according to Proposition 3, then a continuous time dynamic planar system with two unstable foci is determined by (16).*

Proof. A dynamical system given by (5) that fulfills Proposition 3 can be transformed by (11) and expressed as an uncoupled system (14). Then, the linear operator (15) of the planar system is given by the Jordan block related to the complex eigenvalues $\lambda_{2,3} = \alpha \pm i\beta$,

$$A = \begin{pmatrix} \alpha & -\beta \\ \beta & \alpha \end{pmatrix}.$$

The equilibria \mathbf{x}_i^* of the planar system are determined by the equilibria \mathbf{y}_i^* of the uncoupled system, with $i = 1, \dots, \eta$. The components of \mathbf{x}_i^* are given by the form of the linear operator E . If E is given by the first matrix of (13), the second and third components of \mathbf{y}_i^* conform to the components of \mathbf{x}_i^* . In another case, the first and second components of \mathbf{y}_i^* conform to the components of \mathbf{x}_i^* . Therefore, the vectors B_i are given by $-A_i^{-1} \mathbf{x}_i^*$.

The borders l_i of the convex sets D_i , where subsystems (A, B_i) are acting, are given by the lines l_i that pass through the equilibria \mathbf{x}_i^* , and these lines l_i are parallel to the projected line given by the intersection of the plane QSW with the unstable manifold, with $i = 1, \dots, \eta$. \square

As an example, now, we begin to determine the system (14) by considering Example 1 as follows.

Example 2: *Determine a planar PWL system (16) by considering the dynamical system of Example 1.*

The first step is to get the uncoupled system given by (14). Then, under the coordinate transformation given by (11), the matrix Q to obtain an uncoupled system with two atoms in the partition

$\mathcal{P}_y = \{P_{1y}, P_{2y}\}$ is given as follows:

$$Q = \begin{pmatrix} 1 & 0 & -1 \\ 0 & -1 & 0 \\ 1/2 & 0 & 1 \end{pmatrix}.$$

The switching plane QSW that generates the partition $\mathcal{P}_y = \{P_{1y} = \{\mathbf{y} \in \mathbb{R}^3 : \mathbf{y} < \text{QSW} \text{ or } \mathbf{y} \in \text{QSW}^-\}, P_{2y} = \{\mathbf{y} \in \mathbb{R}^3 : \mathbf{y} > \text{QSW} \text{ or } \mathbf{y} \in \text{QSW}^+\}\}$ is

$$\text{QSW} = \{\mathbf{y} \in \mathbb{R}^3 : y_1 - 2y_3 = 0\}, \tag{17}$$

with $\text{QSW}^- = \{\mathbf{y} \in \mathbb{R}^3 : y_1 + y_3 \geq 0\} \cap \text{QSW} \subset P_{1y}$ and $\text{QSW}^+ = \{\mathbf{y} \in \mathbb{R}^3 : y_1 + y_3 < 0\} \cap \text{QSW} \subset P_{2y}$.

The matrix of the linear operator $E \in \mathbb{R}^{3 \times 3}$ given by the first matrix of (13), for the parameters $\alpha = 0.2$, $\beta = 5$, $\gamma = -3$, $\kappa_1 = -1$, and $\kappa_2 = 1$, and the constant vector $Q^{-1}f(Q\mathbf{y})B \in \mathbb{R}^3$ based on the eigenvalues defined in³⁹ are as follows:

$$\begin{pmatrix} \frac{2\gamma}{3} \\ \frac{\beta}{3} \\ -\frac{\alpha}{3} \end{pmatrix} \text{ for } \mathbf{y} \in P_{1y}, \text{ and } \begin{pmatrix} -\frac{2\gamma}{3} \\ -\frac{\beta}{3} \\ \frac{\alpha}{3} \end{pmatrix} \text{ for } \mathbf{y} \in P_{2y}. \tag{18}$$

The functional f is given by

$$f(\mathbf{y}) = \begin{cases} \kappa_1, & \mathbf{y} \in P_{1y}, \\ \kappa_2, & \mathbf{y} \in P_{2y}, \end{cases} \tag{19}$$

with $\kappa_1, \kappa_2 \in \mathbb{R}$. Therefore, the equilibria are at $\mathbf{y}_{eq1}^* = (-2/3, 0, 1/3)^T \in P_{1y}$, and $\mathbf{y}_{eq2}^* = (2/3, 0, -1/3)^T \in P_{2y}$, and the stable and the unstable manifolds are given by

$$W_{\mathbf{y}_{eq1}^*}^u = \{\mathbf{y} \in P_{1y} \subset \mathbb{R}^3 : y_1 = -2/3\}, \tag{20}$$

$$W_{\mathbf{y}_{eq2}^*}^u = \{\mathbf{y} \in P_{2y} \subset \mathbb{R}^3 : y_1 = 2/3\}, \tag{21}$$

$$W_{\mathbf{y}_{eq1}^*}^s = \{\mathbf{y} \in P_{1y} \subset \mathbb{R}^3 : y_2 = 0, y_3 = 1/3\}, \tag{22}$$

$$W_{\mathbf{y}_{eq2}^*}^s = \{\mathbf{y} \in P_{2y} \subset \mathbb{R}^3 : y_2 = 0, y_3 = -1/3\}. \tag{23}$$

The intersection points are given by $cl(W_{\mathbf{y}_{eq1}^*}^s) \cap cl(W_{\mathbf{y}_{eq2}^*}^u) = (-\frac{2}{3}, 0, -\frac{1}{3})^T$ and $cl(W_{\mathbf{y}_{eq1}^*}^u) \cap cl(W_{\mathbf{y}_{eq2}^*}^s) = (\frac{2}{3}, 0, \frac{1}{3})^T$.

The above defined the uncoupled system given by (14) that fulfills Proposition 3; therefore, it presents a heteroclinic orbit [see Fig. 3(a)]. The heteroclinic chaos emerges from this system; in particular, a double-scroll attractor is generated as it is shown in Fig. 3(b), for the following initial condition $\mathbf{y}_0 = (0, 0, 0)^T$, and Fig. 4 shows projections of the attractor onto different planes: (a) (y_1, y_2) , (b) (y_1, y_3) , and (c) (y_2, y_3) .

There are remarkable differences between the displayed projections of Figs. 2(a) and 2(c) and its corresponding projections of Figs. 4(a) and 4(c). Figure 2(a) shows the shape of a double-scroll projected onto the plane (x_1, x_2) ; meanwhile, Fig. 4(a) shows that the shape of the double-scroll is lost. Figure 2(c) shows the shape of a single-scroll projected onto the plane (x_2, x_3) ; meanwhile, Fig. 4(c) shows the shape of a double-scroll projected onto the plane (y_2, y_3) .

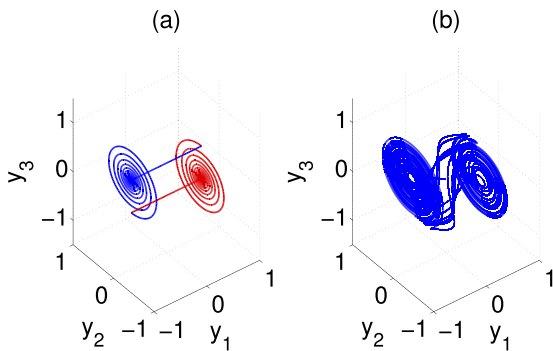


FIG. 3. (a) Heteroclinic cycle, the blue and red trajectories belong to the atoms P_{1y} and P_{2y} , respectively. The heteroclinic orbit from y_{eq1}^* to y_{eq2}^* is comprised of the blue spiral trajectory and the red straight trajectory. Another heteroclinic orbit from y_{eq2}^* to y_{eq1}^* is comprised of the red spiral trajectory and the blue straight trajectory. (b) A double-scroll attractor that emerges from a heteroclinic orbit using the following initial condition $y_0 = (0, 0, 0)^T$ and the parameters $\alpha = 0.2, \beta = 5, \gamma = -3, \kappa_1 = -1, \kappa_2 = 1$ for the system defined by (14) and (6) with the switching surface $QSW = \{y \in \mathbb{R}^3 : y_1 - 2y_3 = 0\}$.

The continuous time dynamic planar system with two unstable foci is given by (15) and (16) by considering the following linear operators:

$$A_1 = A_2 = \begin{pmatrix} 0.2 & -5 \\ 5 & 0.2 \end{pmatrix}. \tag{24}$$

The equilibria of the system are at $x_1^* = (0, 1/3)^T \in D_1$ and $x_2^* = (0, -1/3)^T \in D_2$, where the convex sets are defined as follows:

$$D_1 = \{(x, y) : -1/3 < y \in \mathbb{R}\} \quad \text{and} \quad D_2 = \{(x, y) : y < 1/3 \in \mathbb{R}\}. \tag{25}$$

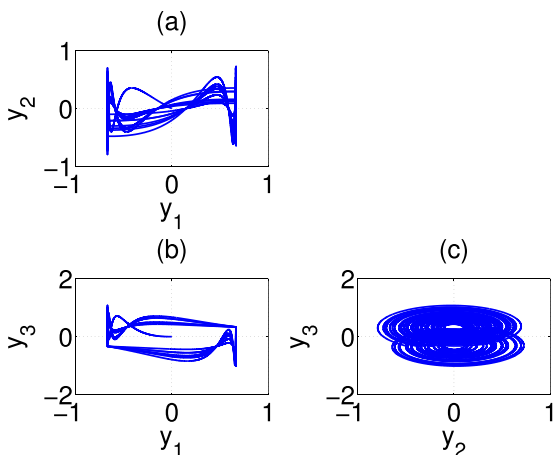


FIG. 4. Projections of the double-scroll attractor on the planes: (a) (y_1, y_2) , (b) (y_1, y_3) , and (c) (y_2, y_3) . The initial condition $y_0 = (0, 0, 0)^T$ and the parameters $\alpha = 0.2, \beta = 5, \gamma = -3, \kappa_1 = -1, \kappa_2 = 1$, for the system defined by (14) and (6) with the switching surface $QSW = \{y \in \mathbb{R}^3 : y_1 - 2y_3 = 0\}$.

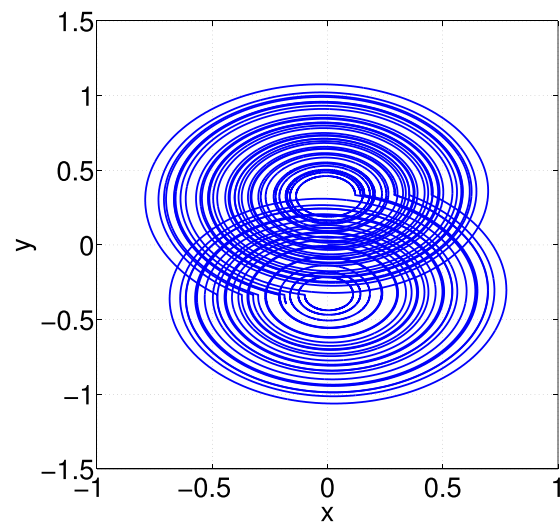


FIG. 5. A double-scroll attractor of the continuous time dynamic planar systems with two unstable foci given by (16) and (24), for the initial condition $x_0 = (0, 0)^T$.

The borders, $l_1 = -1/3$ and $l_2 = 1/3$, of the convex sets D_1 and D_2 , pass through the equilibria x_1^* and x_2^* , respectively. These lines l_1 and l_2 are parallel to the line given by the intersection of the plane QSW (17) and the unstable manifolds given by the planes (20) and (21). Finally, the vectors B_1 and B_2 are defined by $-A_1 x_1^*$ and $-A_2 x_2^*$, respectively,

$$B_1 = \begin{pmatrix} 5/3 \\ -1/15 \end{pmatrix} \quad \text{and} \quad B_2 = \begin{pmatrix} -5/3 \\ 1/15 \end{pmatrix}. \tag{26}$$

We have defined a continuous time dynamic planar system given by (16) and (24)–(26). This planar system presents two unstable foci and uses the hysteresis phenomenon to display a double-scroll attractor. Figure 5 shows a double-scroll attractor for the initial condition $x_0 = (0, 0)^T$. Notice that this attractor is equal to the projection of the attractor of Fig. 4(c).

V. MULTISCROLL ATTRACTORS ON THE PLANE

An approach to generate a one-directional grid multiscroll attractor via a PWL system based on UDS type I was given in³⁸ by defining a double-scroll attractor as follows:

- Consider the linear operator A ,

$$A = \begin{pmatrix} 0 & 1 & 0 \\ 0 & 0 & 1 \\ -\alpha_{31} & -\alpha_{32} & -\alpha_{33} \end{pmatrix}, \tag{27}$$

where α_{31}, α_{32} , and α_{33} satisfy the UDS type I conditions.

- Choose two equilibria on the x -axis: $x_{eq1}^* = (x_{1eq1}^*, 0, 0)^T$ and $x_{eq2}^* = (x_{1eq2}^*, 0, 0)^T$.
- Compute the stable and unstable manifolds $W_{x_{eq1}^*}^s, W_{x_{eq1}^*}^u, W_{x_{eq2}^*}^s$, and $W_{x_{eq2}^*}^u$.

- Find the intersection points between the stable and unstable manifold $W_{x_{eq1}^*}^s \cap W_{x_{eq2}^*}^u$ and $W_{x_{eq2}^*}^s \cap W_{x_{eq1}^*}^u$.
- Define the switching surface SW_{12} as the plane $g_1(\mathbf{x}) = 0$ that passes through the intersection points $W_{x_{eq1}^*}^s \cap W_{x_{eq2}^*}^u$ and $W_{x_{eq2}^*}^s \cap W_{x_{eq1}^*}^u$ and the line: $x_1 = (x_{1eq1}^* + x_{1eq2}^*)/2, x_3 = 0$.
- Define the partition \mathcal{P} by considering $P_1 = \{\mathbf{x} \in \mathbb{R}^3 : \mathbf{x} < SW \text{ or } \mathbf{x} \in SW^-\}$ and $P_2 = \{\mathbf{x} \in \mathbb{R}^3 : \mathbf{x} > SW \text{ or } \mathbf{x} \in SW^+\}$, with the switching plane $SW = SW^- \cup SW^+$, such that $W_{x_{eq1}^*}^s \cap W_{x_{eq2}^*}^u \in P_1$ and $W_{x_{eq2}^*}^s \cap W_{x_{eq1}^*}^u \in P_2$.
- Compute the constant vectors $\kappa_i B = -A\mathbf{x}_{eqi}^*$, with $i = 1, 2$. The κ_i values determine the functional $f(\mathbf{x})$.

The above steps generate two heteroclinic orbits between the equilibria \mathbf{x}_{eq1}^* and \mathbf{x}_{eq2}^* , and then the system (5) fulfills Proposition 3.

Proposition 7: Given a partition $\mathcal{P} = \{P_1, P_2\}$ and the PWL system (5) based on UDS-I that generates a heteroclinic loop according to the above steps between equilibria $\mathbf{x}_{eq1}^* = (x_{1eq1}^*, 0, 0)^T$ and $\mathbf{x}_{eq2}^* = (x_{1eq1}^* + \hat{d}_1, 0, 0)^T$, $\hat{d}_1 \in \mathbb{R}$, with the linear operator defined by (27), $B = (0, 0, 1)$, and the switching surface given by the plane $g_1(\mathbf{x}) = 0$. Then, multiple heteroclinic loops are generated between η equilibria in the partition $\mathcal{P} = \{P_1, \dots, P_\eta\}$, $2 < \eta \in \mathbb{N}$, if the equilibria are given by $\mathbf{x}_{eqi}^* = (x_{1eq1}^* + (i - 1)\hat{d}_1, 0, 0)^T$, with $i = 1, \dots, \eta$, and switching surfaces are given by parallel planes $g_i(\mathbf{x}) = 0$ that pass through the points $((x_{1eq1}^* + x_{1eq(i+1)}^*)/2, 0, 0)^T$, with $i = 1, \dots, \eta - 1$.

Proof. The PWL system (5) is completely determined by the linear operator A , the vectors $\kappa_i B$, the functional $f(\mathbf{x})$, and the partition \mathcal{P} . Proposition 7 states A , B , and \mathcal{P} , and then the functional $f(\mathbf{x})$ needs to be computed as follows.

We have $A * \mathbf{x}_{eq1}^* = (0, 0, -\alpha_{31}x_{1eq1}^*)^T = -f(\mathbf{x})B = (0, 0, -\kappa_1)^T$ for $\mathbf{x} \in P_1$ and $A * \mathbf{x}_{eq2}^* = (0, 0, -\alpha_{31}(x_{1eq1}^* + \hat{d}_1))^T = -f(\mathbf{x})B = (0, 0, -\kappa_1 - \hat{d}_2)^T$ for $\mathbf{x} \in P_2$, and then the functional $f(\mathbf{x}) = \kappa_1$, if $\mathbf{x} \in P_1$, and $f(\mathbf{x}) = \kappa_1 + \hat{d}_2$, if $\mathbf{x} \in P_2$, with $\kappa_1 = \alpha_{31}x_{1eq1}^*$ and $\hat{d}_2 = \alpha_{31}\hat{d}_1$. Therefore, for a partition with η atoms, the functional is given by

$$f(\mathbf{x}) = \kappa_1 + (i - 1)\hat{d}_2, \text{ if } \mathbf{x} \in P_i, \text{ with } i = 1, \dots, \eta.$$

Now, the PWL system (5) is completely defined.

The heteroclinic loops between equilibria \mathbf{x}_{eqi}^* , with $i = 1, \dots, \eta$, are a consequence of the heteroclinic loop between equilibria

$\mathbf{x}_{eq1}^* = (x_{1eq1}^*, 0, 0)^T$ and $\mathbf{x}_{eq2}^* = (x_{1eq1}^* + \hat{d}_1, 0, 0)^T$ because all the equilibria are given by $\mathbf{x}_{eqi}^* = (x_{1eq1}^* + (i - 1)\hat{d}_1, 0, 0)^T$, with $i = 1, \dots, \eta$, and then they are equidistant. Also, switching surfaces are given by parallel planes $g_i(\mathbf{x}) = 0$ and pass through equidistant points $((x_{1eqi}^* + x_{1eq(i+1)}^*)/2, 0, 0)^T$, with $i = 1, \dots, \eta - 1$. Therefore, the pair of equilibria \mathbf{x}_{eqi}^* and $\mathbf{x}_{eq(i+1)}^*$ presents a heteroclinic loop as the pair of equilibria \mathbf{x}_{eq1}^* and \mathbf{x}_{eq2}^* . This completes the proof. \square

The heteroclinic chaos is given in multiscroll attractors by consider the PWL system (5) according to Proposition 7 and Assumption 5.

Example 3: In order to illustrate the generation of multiscroll attractors using (5), we consider a PWL system defined in \mathbb{R}^3 to generate a ten-scroll chaotic attractor with the state vector $\mathbf{x} = (x_1, x_2, x_3)^T$ and the linear operator defined by (27), where $\alpha_{31} = 1.5, \alpha_{32} = 1$, and $\alpha_{33} = 1$.

Thus, the eigenvalues are $\lambda_1 = -1882/1563, \lambda_2 = 319/3126 + 2503/2252i$, and $\lambda_3 = 319/3126 - 2503/2252i$, which satisfy $\sum_{i=1}^3 \lambda_i < 0$ and $\text{Im}(\lambda_2)/\text{Re}(\lambda_2) > 6$. $\text{Im}(\lambda_2)$ and $\text{Re}(\lambda_2)$ denote the imaginary part and real part of λ_2 , respectively.

Choose equilibria at $\mathbf{x}_{eq1}^* = (0, 0, 0)^T, \mathbf{x}_{eq2}^* = (0.6, 0, 0)^T, \mathbf{x}_{eq3}^* = (1.2, 0, 0)^T, \mathbf{x}_{eq4}^* = (1.8, 0, 0)^T, \mathbf{x}_{eq5}^* = (2.4, 0, 0)^T, \mathbf{x}_{eq6}^* = (3, 0, 0)^T, \mathbf{x}_{eq7}^* = (3.6, 0, 0)^T, \mathbf{x}_{eq8}^* = (4.2, 0, 0)^T, \mathbf{x}_{eq9}^* = (4.8, 0, 0)^T$, and $\mathbf{x}_{eq10}^* = (5.4, 0, 0)^T$.

The unstable manifolds are given as follows:

$$W_{x_{eqi}^*}^u = \{\mathbf{x} \in \mathbb{R}^3 : 0.3646x_1 - 0.0597x_2 + 0.2927x_3 - D_i = 0\},$$

with $i = 1, \dots, 10$, and $D_1 = 0, D_2 = 0.2188, D_3 = 0.4375, D_4 = 0.6563, D_5 = 0.8750, D_6 = 1.0938, D_7 = 1.3125, D_8 = 1.5313, D_9 = 1.7500$, and $D_{10} = 1.9688$. The stable manifolds are given by

$$W_{x_{eqi}^*}^s = \left\{ \mathbf{x} \in \mathbb{R}^3 : \frac{x_1 - x_{1eqi}^*}{-0.4687} = \frac{x_2}{0.5644} = \frac{x_3}{-0.6796} \right\},$$

with $i = 1, \dots, 10$. Therefore, the switching surfaces are given by

$$SW_{i(i+1)} = \{\mathbf{x} \in \mathbb{R}^3 : g_i(\mathbf{x}) = 0\}, \text{ with } i = 1, \dots, 9,$$

where $g_i(\mathbf{x}) = 0.7369x_1 + 0.0918x_3 - \hat{D}_i$, with $\hat{D}_1 = 0.2211, \hat{D}_2 = 0.6632, \hat{D}_3 = 1.1054, \hat{D}_4 = 1.5474, \hat{D}_5 = 1.9896, \hat{D}_6 = 2.4318, \hat{D}_7 = 2.8739, \hat{D}_8 = 3.3160$, and $\hat{D}_9 = 3.7582$. The sets $SW_{i(i+1)}^-$ and $SW_{i(i+1)}^+$ are for $x_3 \geq 0$ and $x_3 < 0$, respectively. The set of constant vectors $f(\mathbf{x})B = -A\mathbf{x}_{eqi}^*$, with $i = 1, \dots, 10$, is given by

$$\begin{aligned} f(\mathbf{x})B &= \{\kappa_1 B = (0, 0, 0)^T, \kappa_2 B = (0, 0, 0.9)^T, \kappa_3 B = (0, 0, 1.8)^T, \\ \kappa_4 B &= (0, 0, 2.7)^T, \kappa_5 B = (0, 0, 3.6)^T, \kappa_6 B = (0, 0, 4.5)^T, \kappa_7 B = (0, 0, 5.4)^T, \\ \kappa_8 B &= (0, 0, 6.3)^T, \kappa_9 B = (0, 0, 7.2)^T, \kappa_{10} = (0, 0, 8.1)^T\} \end{aligned}$$

and the partition,

$$\begin{aligned}
 \mathcal{P} = \{ & P_1 = \{\mathbf{x} \in \mathbb{R}^3 : g_1(\mathbf{x}) < 0, \text{ or } \mathbf{x} \in SW_{12}^-\}, \\
 & P_2 = \{\mathbf{x} \in \mathbb{R}^3 : 0 < g_1(\mathbf{x}) \ \& \ g_2(\mathbf{x}) < 0, \text{ or } \mathbf{x} \in SW_{12}^+, \text{ or } \mathbf{x} \in SW_{23}^-\}, \\
 & P_3 = \{\mathbf{x} \in \mathbb{R}^3 : 0 < g_2(\mathbf{x}) \ \& \ g_3(\mathbf{x}) < 0, \text{ or } \mathbf{x} \in SW_{23}^+, \text{ or } \mathbf{x} \in SW_{34}^-\}, \\
 & P_4 = \{\mathbf{x} \in \mathbb{R}^3 : 0 < g_3(\mathbf{x}) \ \& \ g_4(\mathbf{x}) < 0, \text{ or } \mathbf{x} \in SW_{34}^+, \text{ or } \mathbf{x} \in SW_{45}^-\}, \\
 & P_5 = \{\mathbf{x} \in \mathbb{R}^3 : 0 < g_4(\mathbf{x}) \ \& \ g_5(\mathbf{x}) < 0, \text{ or } \mathbf{x} \in SW_{45}^+, \text{ or } \mathbf{x} \in SW_{56}^-\}, \\
 & P_6 = \{\mathbf{x} \in \mathbb{R}^3 : 0 < g_5(\mathbf{x}) \ \& \ g_6(\mathbf{x}) < 0, \text{ or } \mathbf{x} \in SW_{56}^+, \text{ or } \mathbf{x} \in SW_{67}^-\}, \\
 & P_7 = \{\mathbf{x} \in \mathbb{R}^3 : 0 < g_6(\mathbf{x}) \ \& \ g_7(\mathbf{x}) < 0, \text{ or } \mathbf{x} \in SW_{67}^+, \text{ or } \mathbf{x} \in SW_{78}^-\}, \\
 & P_8 = \{\mathbf{x} \in \mathbb{R}^3 : 0 < g_7(\mathbf{x}) \ \& \ g_8(\mathbf{x}) < 0, \text{ or } \mathbf{x} \in SW_{78}^+, \text{ or } \mathbf{x} \in SW_{89}^-\}, \\
 & P_9 = \{\mathbf{x} \in \mathbb{R}^3 : 0 < g_8(\mathbf{x}) \ \& \ g_9(\mathbf{x}) < 0, \text{ or } \mathbf{x} \in SW_{89}^+, \text{ or } \mathbf{x} \in SW_{9(10)}^-\}, \\
 & P_{10} = \{\mathbf{x} \in \mathbb{R}^3 : 0 < g_9(\mathbf{x}), \text{ or } \mathbf{x} \in SW_{9(10)}^+\}.
 \end{aligned} \tag{28}$$

The eigenvalues of A are $\lambda_1 = -1.20$ and $\lambda_{2,3} = 0.10 \pm 1.11i$. By Definition 3, the system is an UDS of Type I. Figure 6(a) shows nine heteroclinic cycles between equilibria \mathbf{x}_{eqi}^* and \mathbf{x}_{eqi+1}^* , with $i = 1, \dots, 9$, and Fig. 6(b) depicts the attractor for the initial condition $\mathbf{x}_0 = (0.07, 0.01, 0.09)^T$. Figure 7 shows the projections of the attractor onto different planes: (a) (x_1, x_2) plane, (b) (x_1, x_3) plane, and (c) (x_2, x_3) plane. We solved this system numerically by using the fourth order Runge–Kutta method with 100 000 time iterations and step-size $h = 0.01$.

The generalization of the idea from a double-scroll to a multi-scroll attractor on the plane is easy if a multiscroll attractor in \mathbb{R}^3 is given. The following proposition warrants the aforementioned comment:

Proposition 8: *If there exists a PWL system (5), which generates a multiscroll heteroclinic chaotic attractor according to Proposition 7 and Assumption 5, then a continuous time dynamic planar system driven by hysteresis with multiple unstable foci is determined by*

$$\dot{\mathbf{x}} = \begin{cases} A_1\mathbf{x} + B_1 & \text{for } f_H(\mathbf{x}) = 1, \\ A_1\mathbf{x} + B_2 & \text{for } f_H(\mathbf{x}) = 2, \\ \vdots & \\ A_1\mathbf{x} + B_\eta & \text{for } f_H(\mathbf{x}) = \eta. \end{cases} \tag{29}$$

Also, the hysteresis is given by the following expression:

$$f_H(\mathbf{x}) = \begin{cases} 1 & \text{while } \mathbf{x} \in D_1, \\ \vdots & \\ \eta & \text{while } \mathbf{x} \in D_\eta. \end{cases} \tag{30}$$

The hysteresis is initialized as follows:

$$f_H(\mathbf{x}_0) = \begin{cases} 1 & \text{for } \mathbf{x}_0 \in D_1, \\ 2 & \text{for } \mathbf{x}_0 \in D_2 - H_1, \\ \vdots & \\ \eta & \text{for } \mathbf{x}_0 \in D_\eta - H_{\eta-1}, \end{cases} \tag{31}$$

where $H_i = D_i \cap D_{i+1}$, with $i = 1, \dots, \eta - 1$.

Proof. Because the system (5) fulfills UDS-I, then the eigenvalues of A_1 are $\lambda_1 = -\gamma$ and $\lambda_{2,3} = \alpha \pm i\beta$, with the corresponding eigenvectors v_1, v_2 , and v_3 . Therefore, the matrix $Q = [v_1 \ v_2 \ v_3]$ exists, and the linear transformation $\mathbf{y} = Q^{-1}\mathbf{x}$ defines the uncoupled system (13). Then, the matrices $A_1 \in \mathbb{R}^{2 \times 2}$ are given by

$$A_1 = \begin{pmatrix} \alpha & -\beta \\ \beta & \alpha \end{pmatrix}.$$

The equilibria $\mathbf{x}_i^* = (x_i^*, y_i^*)^T$ are given by the last two components of $\mathbf{y}_{eqi}^* = Q^{-1}\mathbf{x}_{eqi}^*$, with $i = 1, \dots, \eta$; therefore, the vectors $B_i \in \mathbb{R}^2$ are given by $B_i = -A_1\mathbf{x}_i^*$. Also, the borders of the convex sets D_i , with $i = 1, \dots, \eta$, are given by the lines l_i that pass through the equilibria \mathbf{x}_i^* , and they are parallel to the generated line given by the intersection of the plane QSW_{12} with an unstable manifold, where QSW_{12} is the switching plane SW_{12} transformed by Q . Therefore, the planar system is completely determined. \square

Example 4: *Find the continuous time dynamic planar system (29) driven by hysteresis with multiple unstable foci by considering the PWL system of Example 3.*

The uncoupled system is given by $\dot{\mathbf{y}} = E\mathbf{y} + Q^{-1}f(Q\mathbf{y})B$, where

$$E = \begin{pmatrix} -1.2041 & 0 & 0 \\ 0 & 0.1020 & -1.1115 \\ 0 & 1.1115 & 0.1020 \end{pmatrix} \quad \text{and} \tag{32}$$

$$Q = \begin{pmatrix} -0.4687 & -0.0934 & -0.5046 \\ 0.5644 & -0.5703 & 0.0524 \\ -0.6796 & 0 & 0.6393 \end{pmatrix}.$$

The equilibria are at $\mathbf{y}_{eq1}^* = (0, 0, 0)^T$, $\mathbf{y}_{eq2}^* = (-0.5422, -0.5894, -0.5763)^T$, $\mathbf{y}_{eq3}^* = (-1.0843, -1.1788, -1.1527)^T$, $\mathbf{y}_{eq4}^* = (-1.6265, -1.7682, -1.7290)^T$, $\mathbf{y}_{eq5}^* = (-2.1687, -2.3576, -2.3054)^T$, $\mathbf{y}_{eq6}^* = (-2.7108, -2.9470, -2.8817)^T$, $\mathbf{y}_{eq7}^* = (-3.2530, -3.5364, -3.4581)^T$, $\mathbf{y}_{eq8}^* = (-3.7952, -4.1258, -4.0344)^T$, $\mathbf{y}_{eq9}^* = (-4.3373, -4.7153, -4.6108)^T$, and $\mathbf{y}_{eq10}^* = (-4.8795, -5.3047, -5.1871)^T$.

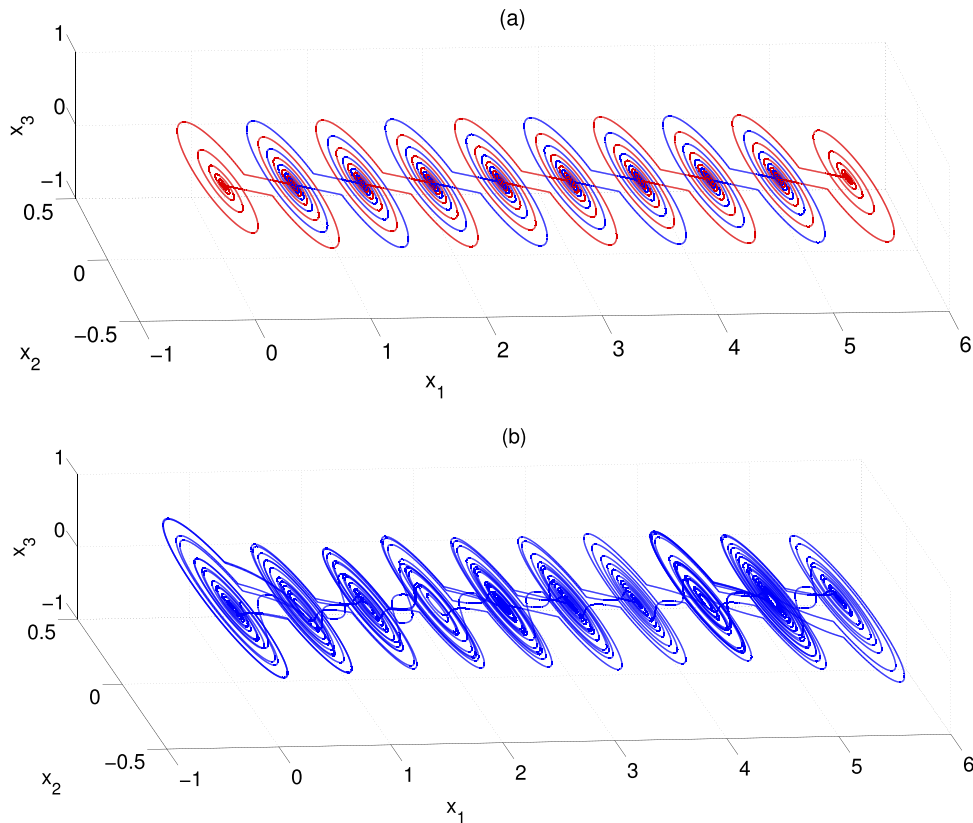


FIG. 6. (a) Nine heteroclinic cycles between equilibria $\mathbf{x}_{eq_i}^*$ and $\mathbf{x}_{eq_{i+1}}^*$, with $i = 1, \dots, 9$. (b) Attractor generated by the quasi-symmetrical 10-PWL(S) system for the initial condition $\mathbf{x}_0 = (0.07, 0.01, 0.09)^T$.

The unstable and stable manifolds are given by $W_{y_{eq_i}^*}^u = \{\mathbf{y} \in \mathbb{R}^3 : y_1 = y_{1eq_i}^*\}$ and $W_{y_{eq_i}^*}^s = \{\mathbf{y} \in \mathbb{R}^3 : y_2 = y_{2eq_i}^*, y_3 = y_{3eq_i}^*\}$, with $i = 1, \dots, 10$, respectively. The switching surfaces QSW are given by $QSW_{i(i+1)} = \{\mathbf{y} \in \mathbb{R}^3 : y_1 + 0.1689y_2 + 0.7679y_3 - 2.4526\hat{D}_i = 0\}$, with $i = 1, \dots, 9$, and $\hat{D}_1 = 0.2211, \hat{D}_2 = 0.6632, \hat{D}_3 = 1.1054, \hat{D}_4 = 1.5474, \hat{D}_5 = 1.9896, \hat{D}_6 = 2.4318, \hat{D}_7 = 2.8739, \hat{D}_8 = 3.3160$, and $\hat{D}_9 = 3.7582$.

The planar system (29) is easily defined by the uncoupled system as follows. The linear operator A_1 is given by

$$A_1 = \begin{pmatrix} 0.1020 & -1.1115 \\ 1.1115 & 0.1020 \end{pmatrix}.$$

The equilibria $\mathbf{x}_i^* \in \mathbb{R}^2$ is given by the second and third components of $\mathbf{y}_{eq_i}^*$, and then the constant vectors $B_i = -A_1 \mathbf{x}_i^*$ are computed as follows:

$$B_1 = \begin{pmatrix} 0 \\ 0 \end{pmatrix}, B_2 = \begin{pmatrix} -0.5809 \\ 0.7144 \end{pmatrix}, B_3 = \begin{pmatrix} -1.1618 \\ 1.4288 \end{pmatrix},$$

$$B_4 = \begin{pmatrix} -1.7426 \\ 2.1432 \end{pmatrix}, B_5 = \begin{pmatrix} -2.3235 \\ 2.8575 \end{pmatrix}, B_6 = \begin{pmatrix} -2.9044 \\ 3.5719 \end{pmatrix},$$

$$B_7 = \begin{pmatrix} -3.4853 \\ 4.2863 \end{pmatrix}, B_8 = \begin{pmatrix} -4.0662 \\ 5.0007 \end{pmatrix}, B_9 = \begin{pmatrix} -4.6470 \\ 5.7151 \end{pmatrix},$$

$$B_{10} = \begin{pmatrix} -5.2279 \\ 6.4295 \end{pmatrix}.$$

The border lines are parallel to the line given by the intersection between the QSW_{12} and $W_{y_{eq_1}^*}^u$. Therefore, the border lines are given by $l_i(\mathbf{x}) = 0.2198x + y + v_i$, with $i = 1, \dots, 10, v_1 = 0, v_2 = 0.7064, v_3 = 1.4127, v_4 = 2.1191, v_5 = 2.8255, v_6 = 3.5318, v_7 = 4.2382, v_8 = 4.9446, v_9 = 5.6510, v_{10} = 6.3573$. Then, the convex sets are given as follows:

$D_1 = \{\mathbf{x} \in \mathbb{R}^2 : l_2(\mathbf{x}) > 0\}$, $D_2 = \{\mathbf{x} \in \mathbb{R}^2 : l_1(\mathbf{x}) < 0 \ \& \ l_3(\mathbf{x}) > 0\}$, $D_3 = \{\mathbf{x} \in \mathbb{R}^2 : l_2(\mathbf{x}) < 0 \ \& \ l_4(\mathbf{x}) > 0\}$, $D_4 = \{\mathbf{x} \in \mathbb{R}^2 : l_3(\mathbf{x}) < 0 \ \& \ l_5(\mathbf{x}) > 0\}$, $D_5 = \{\mathbf{x} \in \mathbb{R}^2 : l_4(\mathbf{x}) < 0 \ \& \ l_6(\mathbf{x}) > 0\}$, $D_6 = \{\mathbf{x} \in \mathbb{R}^2 : l_5(\mathbf{x}) < 0 \ \& \ l_7(\mathbf{x}) > 0\}$, $D_7 = \{\mathbf{x} \in \mathbb{R}^2 : l_6(\mathbf{x}) < 0 \ \& \ l_8(\mathbf{x}) > 0\}$, $D_8 = \{\mathbf{x} \in \mathbb{R}^2 : l_7(\mathbf{x}) < 0 \ \& \ l_9(\mathbf{x}) > 0\}$, $D_9 = \{\mathbf{x} \in \mathbb{R}^2 : l_8(\mathbf{x}) < 0 \ \& \ l_{10}(\mathbf{x}) > 0\}$, and $D_{10} = \{\mathbf{x} \in \mathbb{R}^2 : l_9(\mathbf{x}) < 0\}$.

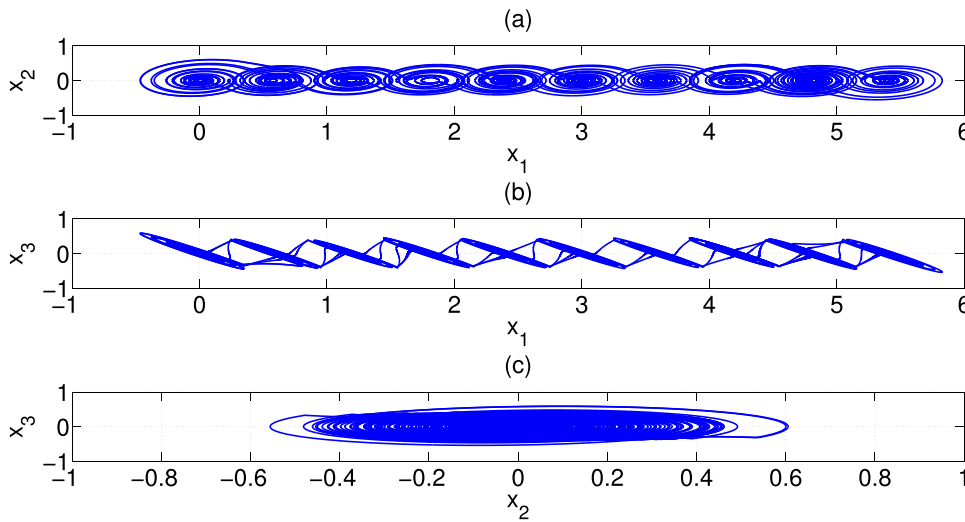


FIG. 7. Projections of the attractor onto different planes: (a) (x_1, x_2) plane, (b) (x_1, x_3) plane, and (c) (x_2, x_3) plane. The initial condition $\mathbf{x}_0 = (0.07, 0.01, 0.09)^T$.

The above convex sets define the hysteresis given by (30), and the initialization is given as follows:

$$f_H(\mathbf{x}_0) = \begin{cases} 1 & \text{for } \mathbf{x}_0 \in D_1, \\ 2 & \text{for } \mathbf{x}_0 \in D_2 - H_1, \\ 3 & \text{for } \mathbf{x}_0 \in D_3 - H_2, \\ 4 & \text{for } \mathbf{x}_0 \in D_4 - H_3, \\ 5 & \text{for } \mathbf{x}_0 \in D_5 - H_4, \\ 6 & \text{for } \mathbf{x}_0 \in D_6 - H_5, \\ 7 & \text{for } \mathbf{x}_0 \in D_7 - H_6, \\ 8 & \text{for } \mathbf{x}_0 \in D_8 - H_7, \\ 9 & \text{for } \mathbf{x}_0 \in D_9 - H_8, \\ 10 & \text{for } \mathbf{x}_0 \in D_{10} - H_9, \end{cases} \quad (33)$$

where $H_1 = D_1 \cap D_2, H_2 = D_2 \cap D_3, H_3 = D_3 \cap D_4, H_4 = D_4 \cap D_5, H_5 = D_5 \cap D_6, H_6 = D_6 \cap D_7, H_7 = D_7 \cap D_8, H_8 = D_8 \cap D_9,$ and $H_9 = D_9 \cap D_{10}$.

Figure 8 shows an attractor with ten scrolls, which is generated by the PWL system (29). Red lines correspond to the border lines l_i , with $i = 1, \dots, 10$. The initial condition is $\mathbf{x}_0 = (-0.1428, 0.0057)^T$.

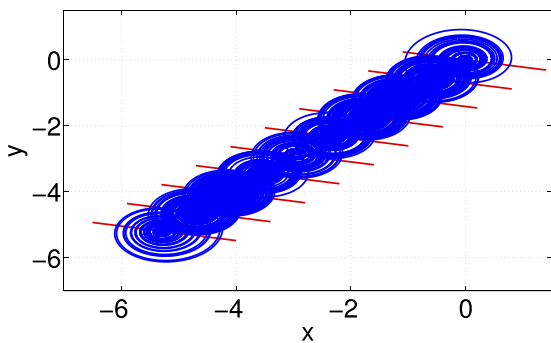


FIG. 8. A ten-scroll attractor given by the PWL system (16) with the initial condition $\mathbf{x}_0 = (-0.1428, 0.0057)^T$. Red lines correspond to the border lines l_i , with $i = 1, \dots, 10$.

VI. CONCLUSION

A class of continuous time PWL systems in \mathbb{R}^2 was derived via PWL systems in \mathbb{R}^3 that generate heteroclinic chaos. This class of continuous time dynamic planar systems presents self-excited attractors with unstable foci. Numerical examples according to the presented theory were given by introducing two systems, the former generates a double-scroll self-excited attractor and the latter is about the generation of a multiscroll self-excited attractor. The approach to generate these kinds of attractors via planar systems and hysteresis allows us to understand an easy generation mechanism and propose new PWL systems in \mathbb{R}^2 .

In this work, we consider only one type of hysteresis, the so-called (delayed) relay, which is the simplest model of discontinuous hysteresis. Now, the dynamics of the systems introduced can be explored through different mathematical expressions of hysteresis.

The problem of designing a hysteresis two-dimensional PWL system with two unstable foci was resolved. The derived hysteresis system captures in some sense the chaotic dynamics of the three-dimensional models. Such dimensional reduction resembles a projection regarding the flow of the three-dimensional system, once putting the system in its Jordan canonical form. This work allows us to ask the following question: is there a topological equivalence between the three-dimensional systems and the hysteresis systems with two unstable foci because this last one can mimic the three-dimensional dynamics? However, the location of the new equilibrium points is altered, becoming on the transition lines.

Furthermore, we believe that this work will help one to find the relationship between the real and imaginary part of a complex eigenvalue $\lambda = \alpha + i\beta$. This is of great interest because heteroclinic chaos always assumes $\alpha \ll \beta$. Also, our future work is to compute the basin of attraction of this class of PWL systems in order to estimate the basin of attraction of a chaotic PWL system in \mathbb{R}^3 .

ACKNOWLEDGMENTS

E. Campos acknowledges CONACYT for the financial support through Project No. A1-S-30433.

REFERENCES

- ¹L. Chua, M. Komuro, and T. Matsumoto, "The double scroll family," *IEEE Trans. Circuits Syst. II* **33**(11), 1072–1118 (1986).
- ²J. A. K. Suykens and J. Vandewalle, "Generation of n-double scrolls ($n = 1, 2, 3, 4, \dots$)," *IEEE Trans. Circuits Syst. I* **40**, 861–867 (1993).
- ³E. Campos-Cantón, J. G. Barajas-Ramírez, G. Solís-Perales, and R. Femat, "Multiscroll attractors by switching systems," *Chaos* **20**(1), 013116 (2010).
- ⁴E. Campos-Cantón, R. Femat, and G. Chen, "Attractors generated from switching unstable dissipative systems," *Chaos* **22**(3), 033121 (2012).
- ⁵R. J. Escalante-González and E. Campos-Cantón, "Generation of chaotic attractors without equilibria via piecewise linear systems," *Int. J. Modern Phys. C* **28**(1), 1750008 (2017).
- ⁶R. J. Escalante-González, E. Campos-Cantón, and M. Nicol, "Generation of multi-scroll attractors without equilibria via piecewise linear systems," *Chaos* **27**, 053109 (2017), 1-82017.
- ⁷R. J. Escalante González and E. Campos Cantón, "A class of piecewise linear systems without equilibria with 3-D grid multiscroll chaotic attractors," *IEEE Trans. Circuits Syst. II* **66**(8), 1456–1460 (2019).
- ⁸G. Huerta Cuellar, E. Jiménez López, E. Campos Cantón, and A. N. Pisarchik, "An approach to generate deterministic Brownian motion," *Commun. Nonlinear Sci. Numer. Simul.* **19**, 2740–2746 (2014).
- ⁹H. E. Gilardi-Velázquez and E. Campos-Cantón, "Non-classical point of view of the Brownian motion generation via fractional deterministic model," *Int. J. Modern Phys. C* **29**(2), 1850020-1–1850020-16 (2018).
- ¹⁰J. Lü and G. Chen, "Generating multiscroll chaotic attractors: Theories, methods and applications," *Int. J. Bifurcation Chaos* **16**(4), 775–858 (2006).
- ¹¹J. Lü, G. Chen, X. Yu, and H. Leung, "Design and analysis of multiscroll chaotic attractors from saturated function series," *IEEE Trans. Circuits Syst. I* **51**(12), 2476–2490 (2004).
- ¹²J. Lü, F. Han, X. Yu, and G. Chen, "Generating 3-D multi-scroll chaotic attractors: A hysteresis series switching method," *Automatica* **40**(10), 1677–1687 (2004).
- ¹³H. E. Gilardi-Velázquez, L. J. Ontañón-García, D. G. Hurtado-Rodríguez, and E. Campos-Cantón, "Multistability in piecewise linear systems versus eigenspectra variation and round function," *Int. J. Bifurcation Chaos* **27**(9), 1730031 (2017).
- ¹⁴A. Anzo-Hernández, H. E. Gilardi-Velázquez, and E. Campos-Cantón, "On multistability behavior of unstable dissipative systems," *Chaos* **28**, 033613 (2018).
- ¹⁵E. Campos Cantón, "Chaotic attractors based on unstable dissipative systems via third-order differential equation," *Int. J. Modern Phys. C* **27**(1), 1650008-1–1650008-11 (2016).
- ¹⁶B. Borem Ferreira, A. Souza de Paula, and M. Amorim Savi, "Chaos control applied to heart rhythm dynamics," *Chaos Solitons Fractals* **44**, 587–599 (2011).
- ¹⁷S. V. Kiyashko, A. S. Pikovsky, and M. I. Rabinovich, "Self-exciting oscillator for the radio-frequency range with stochastic behavior," *Radio Eng. Electron. Phys.* **25**, 2 (1980).
- ¹⁸L. J. Ontañón-García, E. Campos-Cantón, and R. Femat, "Analog electronic implementation of a class of hybrid dissipative dynamical system," *Int. J. Bifurcation Chaos* **26**(01), 1650018 (2016).
- ¹⁹E. Tlelo-Cuautle, A. D. Pano-Azucena, J. J. Rangel-Magdaleno, V. H. Carbajal-Gomez, and G. Rodriguez-Gomez, "Generating a 50-scroll chaotic attractor at 66 MHz by using FPGAs," *Nonlinear Dyn.* **85**(4), 2143–2157 (2016).
- ²⁰A. D. Pano-Azucena, J. J. Rangel-Magdaleno, E. Tlelo-Cuautle, and A. J. Quintas-Valles, "Arduino-based chaotic secure communication system using multi-directional multi-scroll chaotic oscillators," *Nonlinear Dyn.* **87**(4), 2203–2217 (2017).
- ²¹J. M. Muñoz-Pacheco, D. K. Guevara-Flores, O. G. Félix-Beltrán, E. Tlelo-Cuautle, J. E. Barradas-Guevara, and C. K. Volos, "Experimental verification of optimized multiscroll chaotic oscillators based on irregular saturated functions," *Complexity*, **2018**, 3151840.
- ²²T. Zuo, K. Sun, X. Ai, and H. Wang, "High-order grid multiscroll chaotic attractors generated by the second-generation current conveyor circuit," *IEEE Trans. Circuits Syst. II* **61**(10), 818–822 (2014).
- ²³Y. Lin, C. Wang, and L. Zhou, "Generation and implementation of grid multi-scroll hyperchaotic attractors using CCII+," *Optik* **127**(5), 2902–2906 (2016).
- ²⁴H. Mkaouer and O. Boubaker, "Robust control of a class of chaotic and hyperchaotic driven systems," *Pramana J. Phys.* **88**, 9 (2017).
- ²⁵M. García-Martínez, L. J. Ontañón-García, E. Campos-Cantón, and S. Čelikovský, "Hyperchaotic encryption based on multi-scroll piecewise linear systems," *Appl. Math. Comput.* **270**, 413–424 (2015).
- ²⁶M. Esteban, E. Ponce, and F. Torres, "Bifurcation analysis of hysteretic systems with saddle dynamics," *Appl. Math. Nonlinear Sci.* **2**(2), 449–464 (2017).
- ²⁷F. Han, J. Lü, X. Yu, and G. Chen, "Dynamical behaviours of a 3D hysteresis-based system," *Chaos Solitons Fractals* **28**, 182–192 (2006).
- ²⁸X. Yu, F. Han, Y. Feng, and G. Chen, "Domain of attraction of hysteresis-series based chaotic attractors," *Complexity Int.* **12**, 1–10 (2005).
- ²⁹S. Nakagawa and T. Saito, "An RC OTA hysteresis chaos generator," *IEEE Trans. Circuits Syst. I* **43**, 12 (1996).
- ³⁰C. Aissi and D. Kazakos, "An autonomous chaotic CNN hysteresis circuit," *WSEAS Trans. Syst.* **3**(1), 216–220 (2004).
- ³¹S. Nakagawa and T. Saito, "Design and control of RC VCCS 3-D hysteresis chaos generators," *IEEE Trans. Circuits Syst. I* **45**, 2 (1998).
- ³²U. F. Moreno, P. L. D. Peres, and I. S. Bonatti, "Analysis of piecewise-linear oscillators with hysteresis," *IEEE Trans. Circuits Syst. I* **50**, 8 (2003).
- ³³A. N. Pisarchik and R. Jaimes-Reátegui, "Homoclinic orbits in a piecewise linear Rössler-like circuit," *J. Phys. Conf. Ser.* **23**, 122–127 (2005).
- ³⁴R. O. Medrano, M. S. Baptista, and I. L. Caldas, "Homoclinic orbits in a piecewise system and their relation with invariant sets," *Physica D* **186**, 133–147 (2003).
- ³⁵L. Wang and X. S. Yang, "Heteroclinic cycles in a class of 3-dimensional piecewise affine systems," *Nonlinear Anal. Hybrid Syst.* **23**, 44–60 (2017).
- ³⁶G. Li and X. Chen, "Constructing piecewise linear chaotic system based on the heteroclinic Shil'nikov theorem," *Commun. Nonlinear Sci. Numer. Simul.* **14**, 194–203 (2009).
- ³⁷C. Han, F. Yuan, and X. Wang, "Generation method of multipiecewise linear chaotic systems based on the heteroclinic shil'nikov theorem and switching control," *J. Eng.* **2015**, 615187.
- ³⁸A. Anzo-Hernández, E. Campos-Cantón, and M. Nicol, "Itinerary synchronization between PWL systems coupled with unidirectional links," *Commun. Nonlinear Sci. Numer. Simul.* **70**, 102–124 (2019).
- ³⁹R. J. Escalante-González and E. Campos-Cantón, "Coexistence of hidden attractors and self-excited attractors through breaking heteroclinic-like orbits of switched systems," [arXiv:1908.03789](https://arxiv.org/abs/1908.03789) (2019).